Top couplings at the HL-LHC

Lukas Lechner, Daniel Spitzbart, Robert Schöfbeck, Duarte Azevedo, Frédéric Déliot, Andrea Ferroglia, Miguel C. N. Fiolhais, Emanuel Gouveia, António Onofre, Yichen Li, Eleni Vryonidou, Maria Moreno Llacer

1 tt+Z

Many beyond the Standard Model (BSM) predictions include anomalous couplings of the top quark to the electroweak gauge bosons [1–7]. While we restrict this study to the $t\bar{t}Z$ channel and the CMS Phase-2 detector with a luminosity scenario of 3 ab^{-1}, we go beyond earlier work [8] and study the sensitivity of the $t\bar{t}Z$ process using differential cross section data. We interpret the result in terms of the SM effective field theory [9] and set limits on the relevant Wilson coefficients of the Warsaw basis [10] C_{tZ}, $C_{tZ}^{[Im]}$, $C_{\phi t}$ and $C_{\phi Q}$ [11, 12].

1.1 Event simulation

We generate events at the parton level at LO using `MADGRAPH5aMC@NLO` v2.3.3 [13], and decay them using `MadSpin` [14, 15]. Parton showering and hadronization are done using `PYTHIA` 8.2 [16, 17]. Fast detector simulation was performed using `Delphes` [18], with the CMS reconstruction efficiency parametrization for the Phase-2 upgrade. The mean number of interactions per bunch crossing (pileup, PU) is varied from 0 to 200. Jets are reconstructed with the `FastJet` package [19] and using the anti-k_T algorithm [20] with a cone size $R = 0.4$. Besides the signals, we also generate the main backgrounds in the leptonic final states in order to achieve a realistic background prediction. The WZ, tZq, tWZ, $t\bar{t}\gamma$ and $t\bar{t}Z$ processes are normalized to cross sections calculated up to next-to-leading order (NLO) in perturbative QCD.

1.2 Event selection

From results on the inclusive $t\bar{t}Z$ cross section from ATLAS [21, 22] and CMS [23–26] it follows that the three lepton channel, where the Z and one of the W bosons originating from a top quark decay leptonically is the most sensitive search channel. We thus require three reconstructed leptons (e or μ) with $p_T(\ell)$ thresholds of 10, 20, and 40 GeV, respectively, and $|\eta(\ell)| < 3.0$. We furthermore require that there is among them a pair of opposite-sign same-flavor leptons consistent with the Z boson by requiring $|m(\ell\ell) - m_Z| < 10$ GeV. We remove reconstructed leptons within a cone of $\Delta R < 0.3$ to any reconstructed jet satisfying $p_T(j) > 30$ GeV. Furthermore, at least 3 jets are required with $p_T(j) > 30$ GeV and $|\eta(j)| < 4.0$, where one of the jets has been identified as a b-tag jet according to the `Delphes` specification.
We consider the distributions of the observables above in equally sized bins of the transverse Z boson momenta $p_T(Z)$ [27] and $\cos\theta_Z^*$, the relative angle of the negatively charged lepton to the Z boson direction of flight in the rest frame of the boson. The differential cross sections for the SM (black) and BSM (colored lines) interpretations in $t\bar{t}Z$ with respect to $p_T(Z)$ and $\cos\theta_Z^*$ are shown in Fig. 1

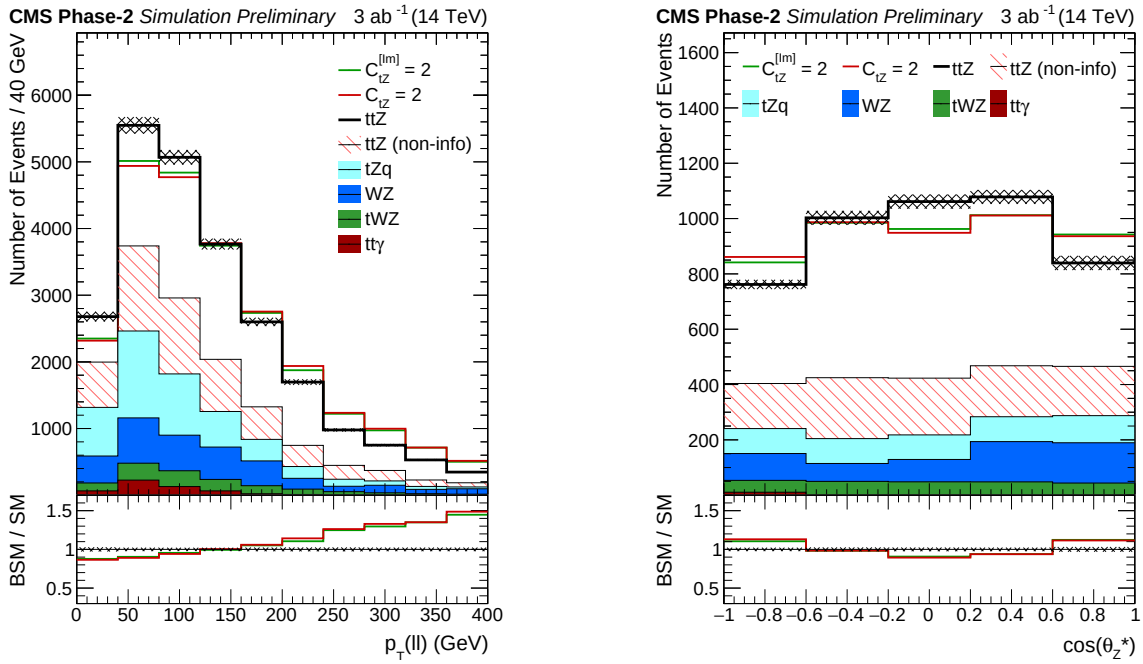

Figure 1: Differential cross sections of $p_T(Z)$ (left) and $\cos\theta^*_Z$ (right) for the in the text mentioned selection and the Phase-2 scenario. For $\cos\theta^*_Z$, additionally $p_T(Z) > 200$ GeV is applied.

for $C_{tZ} = 2\ (\Lambda/\text{TeV})^2$ and $C_{tZ}^{[Im]} = 2\ (\Lambda/\text{TeV})^2$. We normalize the BSM distributions to the SM yield in the plots to visualize the discriminating features of the parameters. The part of the signal which does not contain information on the Wilson coefficients is shown hatched, backgrounds are shown in solid colors.

1.3 Results

The predicted yields are estimated for the 3 ab^{-1} HL-LHC scenario at $\sqrt{s} = 13$ TeV and scaled to 14 TeV, where an additional small background from non-prompt leptons is taken from Ref. [26] and scaled to 3 ab^{-1}. We perform a profiled maximum likelihood fit of the binned likelihood function $L(\theta)$ and consider $q(r) = -2\log(L(\hat{\theta})/L(\hat{\theta}_{SM}))$, where $\hat{\theta}$ and $\hat{\theta}_{SM}$ are the set of nuisance parameters maximizing $L(\theta)$ at the BSM and SM point, respectively. Experimental uncertainties are estimated based on the expected performance of the Phase-2 CMS detector. In Table 1, the 68% and 95% CL intervals of the likelihood scan for the $t\bar{t}Z$ process is shown, where we consider one non-zero Wilson coefficient at a time, and all others are set to zero. In Table 2, we show the 68% and 95% CL intervals of the likelihood ratios for two pairs of Wilson coefficients corresponding to modified neutral current interactions ($C_{\phi t}$ and $C_{\phi Q}$) and dipole moment interactions (C_{tZ} and $C_{tZ}^{[Im]}$). The corresponding second Wilson coefficient is included in the profiling of nuisance parameters. In Fig. 2, the log-likelihood scan for the $t\bar{t}Z$ process is shown in the $C_{\phi Q}/C_{\phi t}$ parameter plane (left) and the dipole moment parameter plane $C_{tZ}/C_{tZ}^{[Im]}$ (right). The green (red) lines show the 68% (95%) CL contour line and the SM parameter point corresponds to $C_{\phi t} = C_{\phi Q} = 0$ and $C_{tZ} = C_{tZ}^{[Im]} = 0$.

Table 1: Expected 68 % and 95 % CL intervals, where one Wilson coefficient at a time is considered non-zero.

Wilson coefficient	68 % CL $(\Lambda/\text{TeV})^2$	95 % CL $(\Lambda/\text{TeV})^2$
$C_{\phi t}$	[-0.47, 0.47]	[-0.89, 0.89]
$C_{\phi Q}$	[-0.38, 0.38]	[-0.75, 0.73]
C_{tZ}	[-0.37, 0.36]	[-0.52, 0.51]
$C_{tZ}^{[Im]}$	[-0.38, 0.36]	[-0.54, 0.51]

Table 2: Expected 68 % and 95 % CL intervals for the selected Wilson coefficients in a profiled scan over the 2D parameter planes $C_{\phi Q}/C_{\phi t}$ and $C_{tZ}/C_{tZ}^{[Im]}$. The respective second parameter of the scan is left free.

Wilson coefficient	68 % CL $(\Lambda/\text{TeV})^2$	95 % CL $(\Lambda/\text{TeV})^2$
$C_{\phi t}$	[-1.65, 3.37]	[-2.89, 6.76]
$C_{\phi Q}$	[-1.35, 2.92]	[-2.33, 6.69]
C_{tZ}	[-0.37, 0.36]	[-0.52, 0.51]
$C_{tZ}^{[Im]}$	[-0.38, 0.36]	[-0.54, 0.51]

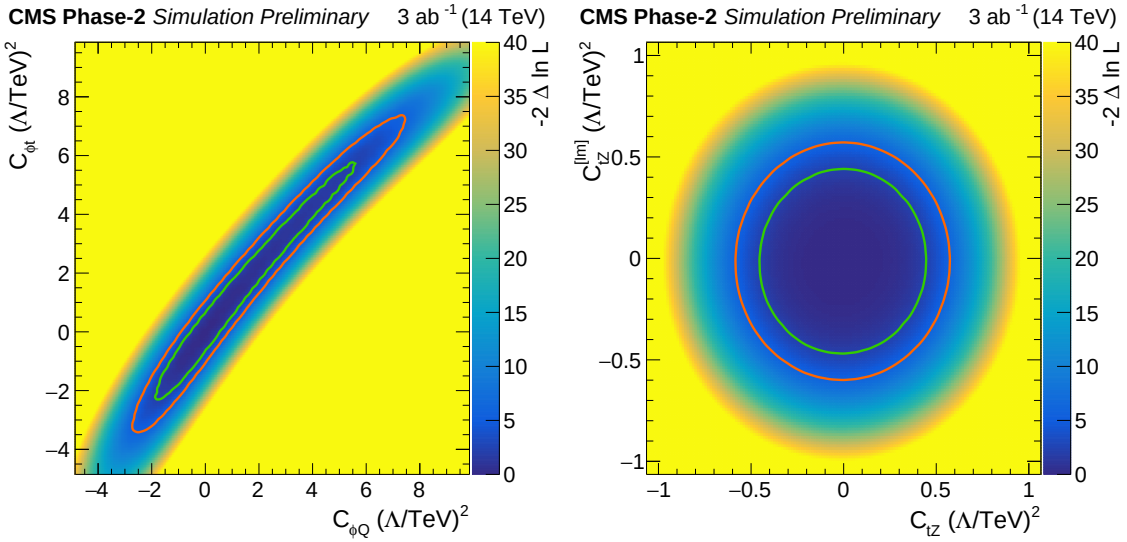

Figure 2: Scan of the negative likelihood in the $C_{\phi Q}/C_{\phi t}$ (left) and $C_{tZ}/C_{tZ}^{[Im]}$ parameter planes (right) for the $t\bar{t}Z$ process under the SM hypothesis. The 68% (95%) CL contour lines are given in green (red).

References

[1] W. Hollik, J. I. Illana, S. Rigolin, C. Schappacher, and D. Stockinger, "Top dipole form-factors and loop induced CP violation in supersymmetry," *Nucl. Phys.* **B551** (1999) 3, arXiv:hep-ph/9812298. [Erratum: Nucl. Phys.B557,407(1999)].

[2] K. Agashe, G. Perez, and A. Soni, "Collider Signals of Top Quark Flavor Violation from a Warped Extra Dimension," *Phys. Rev.* **D75** (2007) 015002.

[3] A. L. Kagan, G. Perez, T. Volansky, and J. Zupan, "General Minimal Flavor Violation," *Phys. Rev.* **D80** (2009) 076002.

[4] T. Ibrahim and P. Nath, "The Top quark electric dipole moment in an MSSM extension with vector like multiplets," *Phys. Rev.* **D82** (2010) 055001.

[5] T. Ibrahim and P. Nath, "The Chromoelectric Dipole Moment of the Top Quark in Models with Vector Like Multiplets," *Phys. Rev.* **D84** (2011) 015003.

[6] C. Grojean, O. Matsedonskyi, and G. Panico, "Light top partners and precision physics," *JHEP* **10** (2013) 160.

[7] F. Richard, "Can LHC observe an anomaly in $t\bar{t}Z$ production?," arXiv:1304.3594.

[8] R. Roentsch and M. Schulze, "Probing top-Z dipole moments at the LHC and ILC," *JHEP* **08** (2015) 044, arXiv:1501.05939 [hep-ph].

[9] D. Barducci *et al.*, "Interpreting top-quark LHC measurements in the standard-model effective field theory," arXiv:1802.07237 [hep-ph].

[10] B. Grzadkowski, M. Iskrzynski, M. Misiak, and J. Rosiek, "Dimension-Six Terms in the Standard Model Lagrangian," *JHEP* **10** (2010) 085, arXiv:1008.4884 [hep-ph].

[11] J. Brehmer, K. Cranmer, F. Kling, and T. Plehn, "Better Higgs boson measurements through information geometry," *Phys. Rev.* **D95** no. 7, (2017) 073002, arXiv:1612.05261 [hep-ph].

[12] J. Brehmer, *New Ideas for Effective Higgs Measurements*. PhD thesis, U. Heidelberg (main), 2017. http://www.thphys.uni-heidelberg.de/~plehn/includes/theses/brehmer_d.pdf.

[13] J. Alwall, R. Frederix, S. Frixione, V. Hirschi, F. Maltoni, O. Mattelaer, H. S. Shao, T. Stelzer, P. Torrielli, and M. Zaro, "The automated computation of tree-level and next-to-leading order differential cross sections, and their matching to parton shower simulations," *JHEP* **07** (2014) 079, arXiv:1405.0301 [hep-ph].

[14] P. Artoisenet, R. Frederix, O. Mattelaer, and R. Rietkerk, "Automatic spin-entangled decays of heavy resonances in Monte Carlo simulations," *JHEP* **03** (2013) 015, arXiv:1212.3460 [hep-ph].

[15] S. Frixione, E. Laenen, P. Motylinski, and B. R. Webber, "Angular correlations of lepton pairs from vector boson and top quark decays in Monte Carlo simulations," *JHEP* **04** (2007) 081, arXiv:hep-ph/0702198 [HEP-PH].

[16] T. Sjöstrand, S. Mrenna, and P. Z. Skands, "A brief introduction to PYTHIA 8.1" *Comput. Phys. Commun.* **178** (2008) 852, arXiv:0710.3820 [hep-ph].

[17] T. Sjöstrand, S. Ask, J. R. Christiansen, R. Corke, N. Desai, P. Ilten, S. Mrenna, S. Prestel, C. O. Rasmussen, and P. Z. Skands, "An introduction to PYTHIA 8.2" *Comput. Phys. Commun.* **191** (2015) 159, arXiv:1410.3012 [hep-ph].

[18] **DELPHES 3** Collaboration, J. de Favereau, C. Delaere, P. Demin, A. Giammanco, V. Lemaître, A. Mertens, and M. Selvaggi, "DELPHES 3, A modular framework for fast simulation of a generic collider experiment," *JHEP* **02** (2014) 057, arXiv:1307.6346 [hep-ex].

[19] M. Cacciari, G. P. Salam, and G. Soyez, "FastJet User Manual," *Eur.Phys.J.* **C72** (2012) 1896, arXiv:1111.6097 [hep-ph].

[20] M. Cacciari, G. P. Salam, and G. Soyez, "The Anti-k(t) jet clustering algorithm," *JHEP* **0804** (2008) 063, arXiv:0802.1189 [hep-ph].

[21] **ATLAS** Collaboration, G. Aad *et al.*, "Measurement of the $t\bar{t}W$ and $t\bar{t}Z$ production cross sections in pp collisions at $\sqrt{s} = 8$ TeV with the ATLAS detector," *JHEP* **11** (2015) 172, arXiv:1509.05276 [hep-ex].

[22] **ATLAS** Collaboration, A. Collaboration, "Measurement of the $t\bar{t}Z$ and $t\bar{t}W$ production cross sections in multilepton final states using 3.2 fb^{-1} of pp collisions at $\sqrt{s} = 13$ TeV with the ATLAS detector," *Eur. Phys. J. C* **77** (2017) 40, arXiv:1609.01599 [hep-ex].

[23] **CMS** Collaboration, S. Chatrchyan *et al.*, "Measurement of associated production of vector bosons and $t\bar{t}$ in pp collisions at $\sqrt{s} = 7TeV$," *Phys. Rev. Lett.* **110** (2013) 172002, 1303.3239.

[24] **CMS** Collaboration, V. Khachatryan *et al.*, "Measurement of top quark-antiquark pair production in association with a W or Z boson in pp collisions at $\sqrt{s} = 8$ TeV," *Eur. Phys. J. C* **74** (2014) 3060, arXiv:1406.7830 [hep-ex].

[25] **CMS** Collaboration, V. Khachatryan *et al.*, "Observation of top quark pairs produced in association with a vector boson in pp collisions at $\sqrt{s} = 8$ TeV," *JHEP* **01** (2016) 096, arXiv:1510.01131 [hep-ex].

[26] **CMS** Collaboration, A. M. Sirunyan *et al.*, "Measurement of the cross section for top quark pair production in association with a W or Z boson in proton-proton collisions at $\sqrt{s} = 13$ TeV," *JHEP* **08** (2018) 011, arXiv:1711.02547 [hep-ex].

[27] R. Roentsch and M. Schulze, "Constraining couplings of top quarks to the Z boson in $t\bar{t}$ + Z production at the LHC," *JHEP* **07** (2014) 091, arXiv:1404.1005 [hep-ph]. [Erratum: JHEP09,132(2015)].